Proc. Indian Acad. Sci. (Earth Planet. Sci.), Vol. 102, No. 2, June 1993, pp. 383–398.

Fine structure of seismotectonics in western Shillong massif, north east India

S MUKHOPADHYAY, R CHANDER and K N KHATTRI
Department of Earth Sciences, University of Roorkee, Roorkee 247 667, India

MS received 11 November 1992; revised 10 March 1993

Abstract. The epicentral tract of the great Assam earthquake of 1897 of magnitude 8·7 was monitored for about 6 months using an array of portable seismographs. The observed seismicity pattern shows several diversely-oriented linear trends, some of which either encompass or parallel known geological faults. A vast majority of the recorded micro-earthquakes had estimated focal depths between 8–14 km. The maximum estimated depth was 45 km. On the basis of a seismic velocity model for the region reported recently and these depth estimates we suggest that the rupture zone of the great 1897 earthquake had a depth of 11–12 km under the western half of the Shillong massif. Four composite fault plane solutions define the nature of dislocation in three of the seismic zones. Three of them show oblique thrusting while one shows pure dip slip reverse faulting. The fault plane solutions fit into a regional pattern of a belt of earthquakes extending in NW-SE direction across the north eastern corner of the Bengal basin. The maximum principle stress axis is approximately NS for all the solutions in conformity with the inferred direction of the Indian-EuroAsian plate convergence in the eastern Himalaya.

Keywords. Shillong massif; seismotectonics; seismicity; 1897 great Assam earthquake; stress pattern.

1. Introduction

The north east India and its surroundings constitute a tectonically complex region (figure 1) characterized by complex geology, a relatively high and spatially nonuniform seismicity, and conspicuous gravity anomalies (Evans 1964; Verma and Mukhopadhyay 1977; Khattri *et al* 1992). It comprises of distinct tectonic units such as the eastern Himalaya, the Arakan Yoma ranges, the Bramhaputra basin, the Shillong massif, the Mikir hills, and the Kopili graben. Each of these units should be investigated in detail using various geophysical and geological methods for a detailed picture of the tectonic processes operating in these regions. Thus our group has operated a portable seismograph array in and around the Shillong massif. In the first half of 1984 this array was operated in the epicentral tract of the great Assam earthquake of 1897 (figures 1 and 2). The results of the analysis of these data presented here include:

- The complex seismicity pattern in the epicentral tract of the great Assam earthquake of 1897 in the western part of Shillong massif (figure 1).
- The possible depth of the fault along which slip may have occurred during this earthquake.
- The regional stress pattern.
- A tectonic model for the area is also proposed.

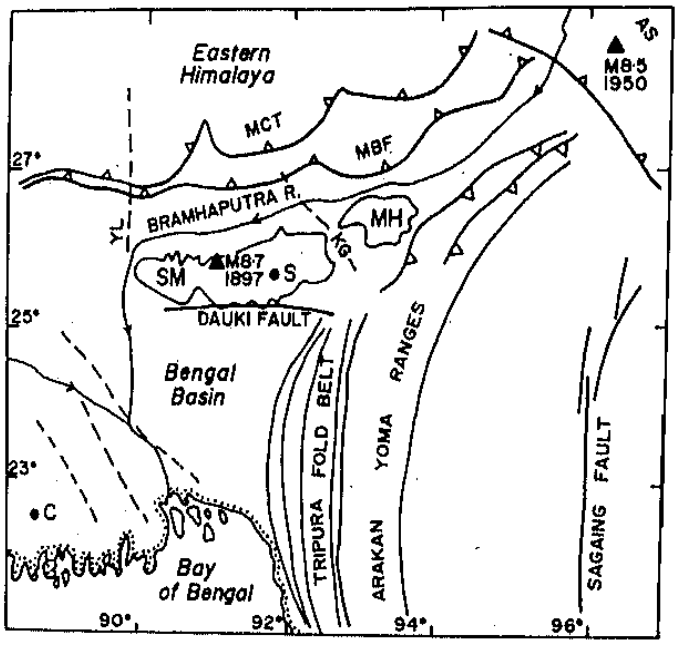

Figure 1. Tectonic and other important features of north eastern India and its surroundings. Abbreviations: R – river; MCT – main central thrust, MBF – main boundary fault, YL – Yamuna lineament, SM – Shillong massif, MH – Mikir hills, KG – Kopili graben, AS – Assam syntaxis, S – Shillong, C – Calcutta. Location of earthquakes with magnitude greater than 8 are shown by triangles. Their magnitude and year of occurrence are shown in the figure.

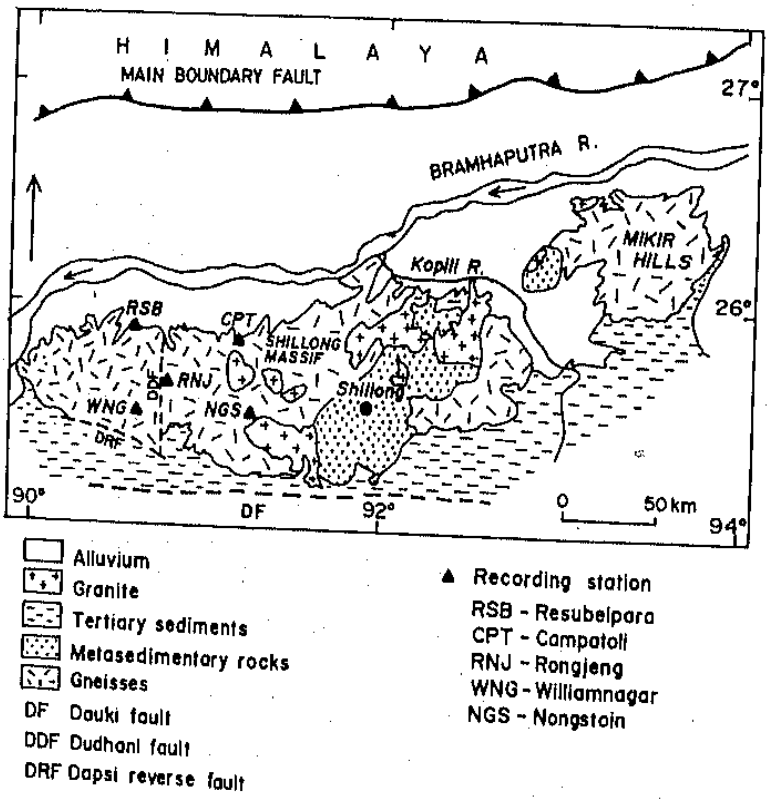

Figure 2. Geological map of the Shillong massif. Locations of the microearthquake array stations are shown by filled triangles.

2. Tectonic set up of Shillong massif

The Shillong massif-Mikir hills ensemble shows very high seismicity, small but conspicuous positive Bouguer anomaly. It has compositional affinity to the Indian craton. The Shillong massif is composed of intensely folded Precambrian metamorphic rocks (figure 2). Numerous N-S, NW-SE, as well as NE-SW trending faults and fractures criss-cross the massif. The massif slopes gently below the sediments of the Bramhaputra river basin to its north. In this area of the basin the molasse deposits show schuppen structure (Murthy *et al* 1971). It is separated from the alluvial plains of Bengal to its south by the almost vertical east–west extending Dauki fault. Just south of Dauki fault overturned Mesozoic and Tertiary sediments are present (GSI 1974; Pascoe 1950; Auden 1972). On the eastern and the western sides of the massif lie respectively the Kopili river graben and the sediments of Garo-Rajmahal gap.

3. Review of available tectonic models of Shillong massif

Various tectonic models for the Shillong massif have been proposed. We review them briefly in this section.

3.1 *Models based on geological data*

Evans (1964) postulated that the massif is an allochthonous body that has moved horizontally eastward along the Dauki fault from the region of Rajmahal trap in Bihar by about 200-250 km to its present position during the Mio-Pliocene period.

Several workers (Murthy 1970; Murthy *et al* 1971; Auden 1972) proposed that it is an autochthonous body that has been rising as a horst since at least the Eocene.

3.2 *Models based on Bouguer gravity data*

Verma and Mukhopadhyay (1977) used the Pratt-Hayford isostatic model for data interpretation and proposed that a 45 km thick high density (2·93 g/cc) crust underlies the Shillong massif. Gupta and Sen (1988) proposed that this high density is due to mafic intrusions in the crust. Khattri *et al* (1992) proposed that the small positive Bouguer anomaly is due to the lateral density contrast caused by the juxtaposition of the crystalline basement rocks in the massif beside the 10–12 km thick sedimentary layer in the Bengal basin. Mukhopadhyay (1990) proposed that since the massif is of small dimension (roughly 250 km by 100 km) the lithosphere may hold it elastically and it need not be isostatically compensated. Chen and Molnar (1990) proposed that the massif remains uncompensated and it is underthrusted by the Indian lithosphere. Gehalaut and Chander (1992) propose that this small positive Bouguer anomaly may have been caused by the presence of a small localized feature within the crust, e.g. a steeply dipping dyke.

3.3. *Models based on Oldham's report on the 1897 great Assam earthquake*

On the basis of Oldham's report several workers (Oldham 1899; Seeber *et al* 1981; Molnar 1987; Khattri 1987; Gehalaut and Chander 1992) have reported that the 1897 great Assam earthquake of magnitude 8·7 occurred along a gently north dipping

thrust plane. Seeber *et al* (1981) proposed that the slip during this earthquake occurred over a 550 km long E-W extending fault. Others opine that this length could not be more than 250 km.

Molnar (1987) proposed that the massif shares with the eastern Himalaya the effect of convergence of India with Eurasia. Khattri *et al* (1992) propose that the massif is overthrusting towards south along the above mentioned fault plane.

Oldham (1899) proposed that the 1897 earthquake may have occurred around 15 km (9·3 miles) depth. In the present work with the help of an independent data set we try to find the probable depth of the related fault plane as well as the type of tectonic stress the massif experiences.

4. Present work

4.1 *Data analysis*

Five portable seismographs were operated in the first half of 1984 in the epicentral tract of this earthquake by our department (figure 2). Teledyne Geotech portacorders (model RV320) and the portable short period (1 Hz) vertical component seismometers S-13 were used. Recordings were made on smoked papers mounted on recording drums. The recorders had internal quartz clocks which were synchronized daily with the radio time signals of atomic time announcements broadcast from the National Physical Laboratory, New Delhi. Time signals were impinged every second on the seismograms. The minimum error with which phases could be picked were 0·2s for P phase and 0·5s for S phase. Both phases were exceptionally clear.

The area showed a very high level of microearthquake activity during this period. On an average 20 microearthquakes were recorded per day. On some days as many as 40 events were recorded at some stations. The best recorded events were used for estimation of the upper crustal velocity structure (Mukhopadhyay 1990) of this area using the Wadati (1933), the Riznichenko (1958), and the Bune's (refer Nicholson and Simpson 1985) methods in conjunction. This velocity structure (table 1) was used for locating all the recorded events. The results are discussed in the following paragraphs.

A total of 670 (out of 1138 recorded over a three-month period from mid-December

Table 1. Velocity model of the Shillong massif used for relocating the microearthquakes that occurred during the early part of 1984. Velocity for the top 26 km is as estimated by us (Mukhopadhyay 1990). Below that depth level the velocity estimated by Kharshiing (1985) was used. The second layer is actually a heterogeneous zone extending from 11·5 km to 26 km depth. The velocity value is an average one for this zone.

Depth to top of layer (km)	Velocity (km/s)
0·0	5·9
11·5	6·3
26·0	6·75
45·0	8·08

1983 to mid-March 1984) microearthquakes were located. The program HYPO71 (Lee and Lahr 1975) was used for locating the events. The average error in epicentral location was 1·8 km and that in the depth of focus was about 3 km for events occurring within the array. The percentage of events showing rms error less than 0·25s, between 0·25 to 0·5s, between 0·5 to 1·0s, and greater than 1·0s are 50, 27, 13 and 10 respectively.

4.2 *Seismicity of the Shillong massif*

Figure 3a shows all the earthquakes with rms error less than 1.0s located within 25°N to 27°N latitude and 90°E to 92°E longitude. The geologically mapped faults and lineaments (GSI 1974; Kayal 1987; Nandy and Dasgupta 1986) are superposed on the seismicity map. From the reported seismicity we infer a WNW-ESE trend crisscrossed by a number of diversely oriented linear zones defined by the epicenters. They show up more prominently when microearthquakes with rms error less than 0·25s are plotted. These zones are shown in figure 3b by thin numbered lines. The most prominent among them are discussed below. A composite L-shaped zone of intense activity is observed within the array (zones 1 and 2). The N-S arm of this zone (zone 2) coincides broadly with the southern part of the Dudhani fault. Whether the northern part of this fault is actually quiet or the apparent lack of seismicity in

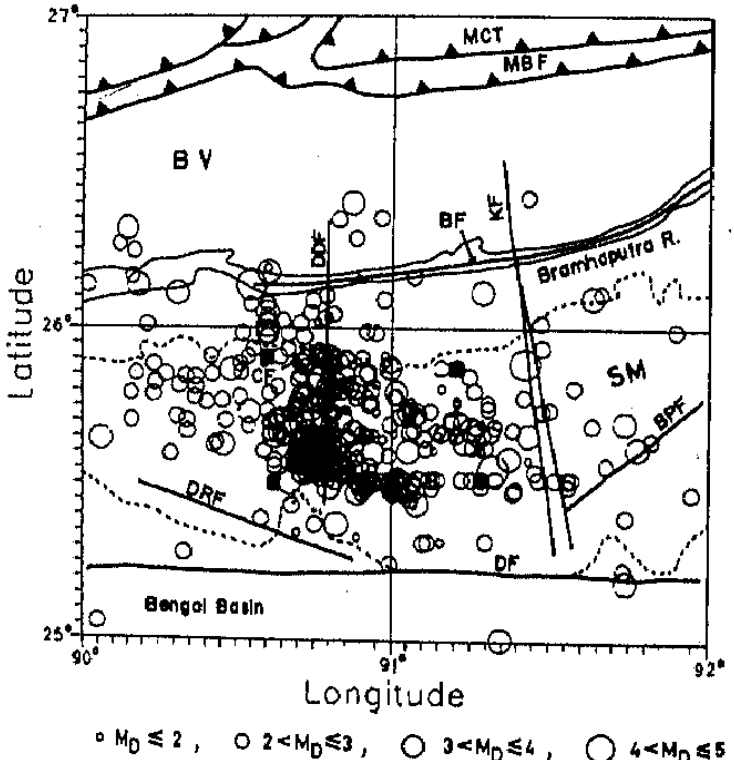

Figure 3a. Epicentral location of microearthquakes recorded during January to March 1984. Locations with rms travel time error $\leq 1{\cdot}0$s are shown. Filled squares represent recording stations. Circles represent microearthquakes. Dashed line shows boundary of the Shillong massif. Abbreviations: SM – Shillong massif; DF – Dauki fault; DRF – Dapsi reverse fault; DDF – Dudhani fault; KF – Kulsi fault; BF – Bramhaputra fault; MCT – main central thrust; MBF – main boundary fault; CF – Chedrang fault; SF – Samin fault, and BV – Bramhaputra valley.

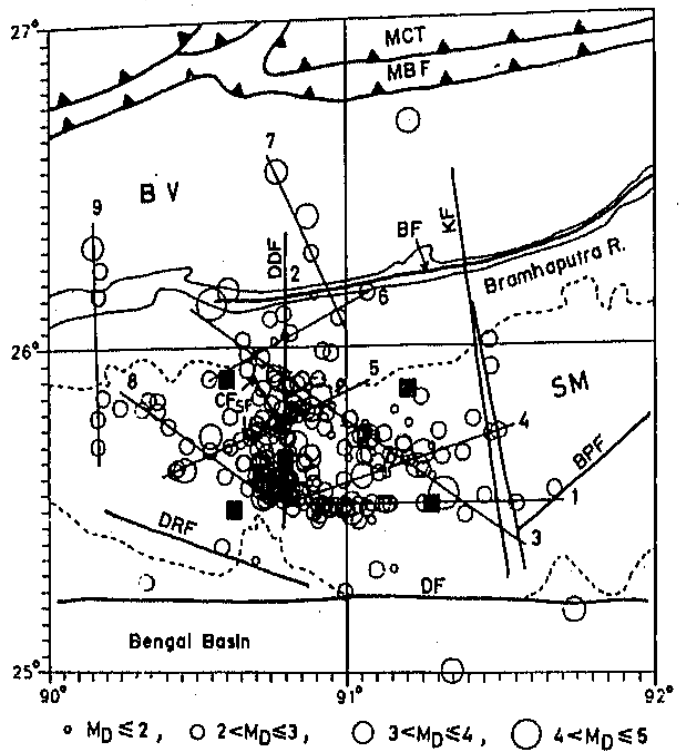

Figure 3b. Epicentral location of microearthquakes recorded during January to March 1984. Only the best quality locations with rms travel time error $\leq 0{\cdot}25$s are shown. Legend as in figure 3a. The epicentral trends are shown with thin numbered lines.

that area is an artifact of lack of adequate coverage is not known. The E-W trend (zone 1) parallels the Dauki fault and lies about 25–30 km towards north of it. To the NE of this L-shaped zone another linear trend (zone 3) of epicenters is seen. It is parallel to the Dapsi reverse fault (figure 3b) and offset from it towards NE by about 50 km. There is earthquake activity in the region outside these three trends also. Some of these epicenters define minor linear trends (figure 3b). Among them linear zones 4, 5, and 6 are almost parallel to each other and trend in the NE direction. The linear zones 3, 7, and 8 are almost parallel to the Dapsi reverse fault (trend SE-NW). Zone 2 is intersected by several linear trends of epicentral plots (lines 3, 4, 5, 6, 8 etc.) and defines a zone of intense microearthquake activity. This zone encompasses the Dudhani fault (figure 2). The topographic map shows marked decrease in elevation in this area compared to its surroundings. Therefore there is a surface expression of tectonic activity going on at a deeper level. This fact is also corroborated by the seismicity map given by Kayal (1987).

4.3 *The depth sections*

The map plot of epicenters reflects the complex tectonic processes operative in the massif. We now examine the depth sections for the separate linear epicentral zones to find out an additional pattern in the seismicity if any.

Figure 4a shows the E-W depth section (1:1) of the earthquakes occurring along the E-W trend of epicenters (zone 1) in figure 3b. The depth section shows a thin linear trend of hypocenters at a depth range between 11·5 and 13 km. As the initial

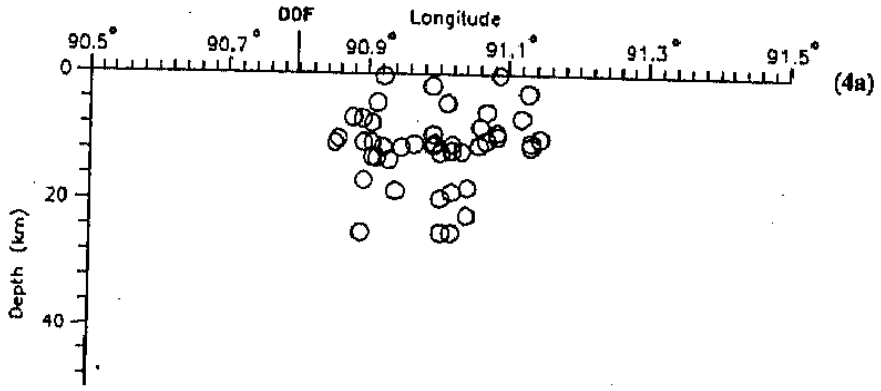
DDF
Longitude
90.5°
90.7°
90.9°
91.1°
91.3°
91.5°
0
20
40
Depth (km)

(4a)

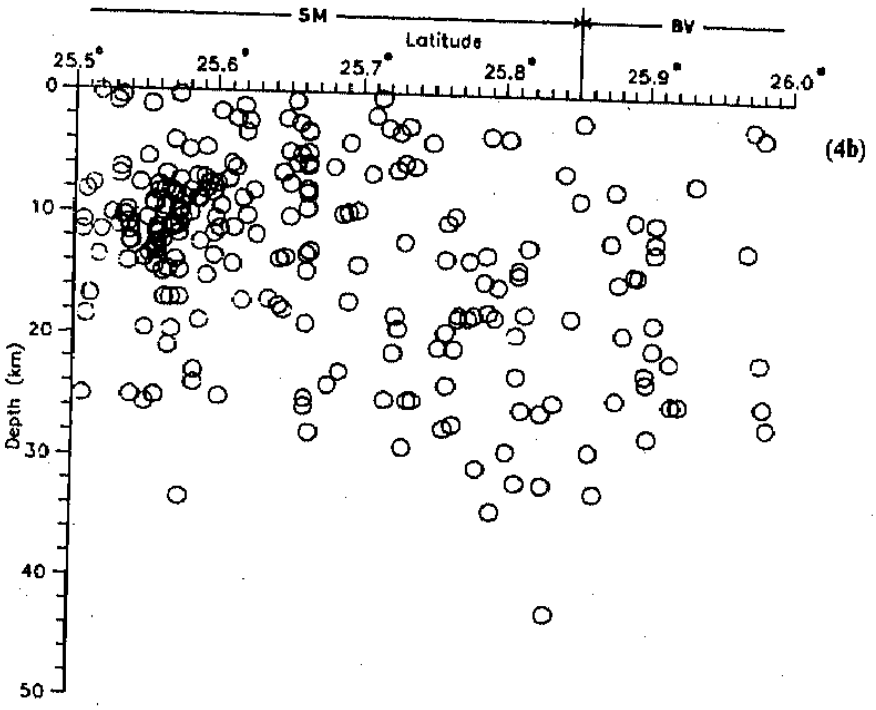
SM
BV
Latitude
25.5°
25.6°
25.7°
25.8°
25.9°
26.0°
0
10
20
30
40
50
Depth (km)

(4b)

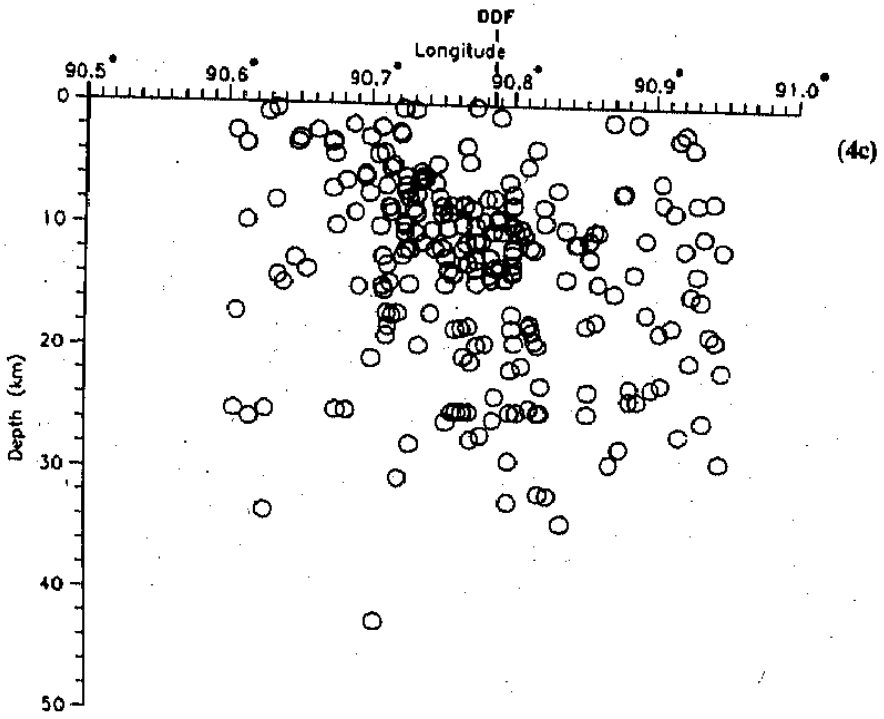
DDF
Longitude
90.5°
90.6°
90.7°
90.8°
90.9°
91.0°
0
10
20
30
40
50
Depth (km)

(4c)

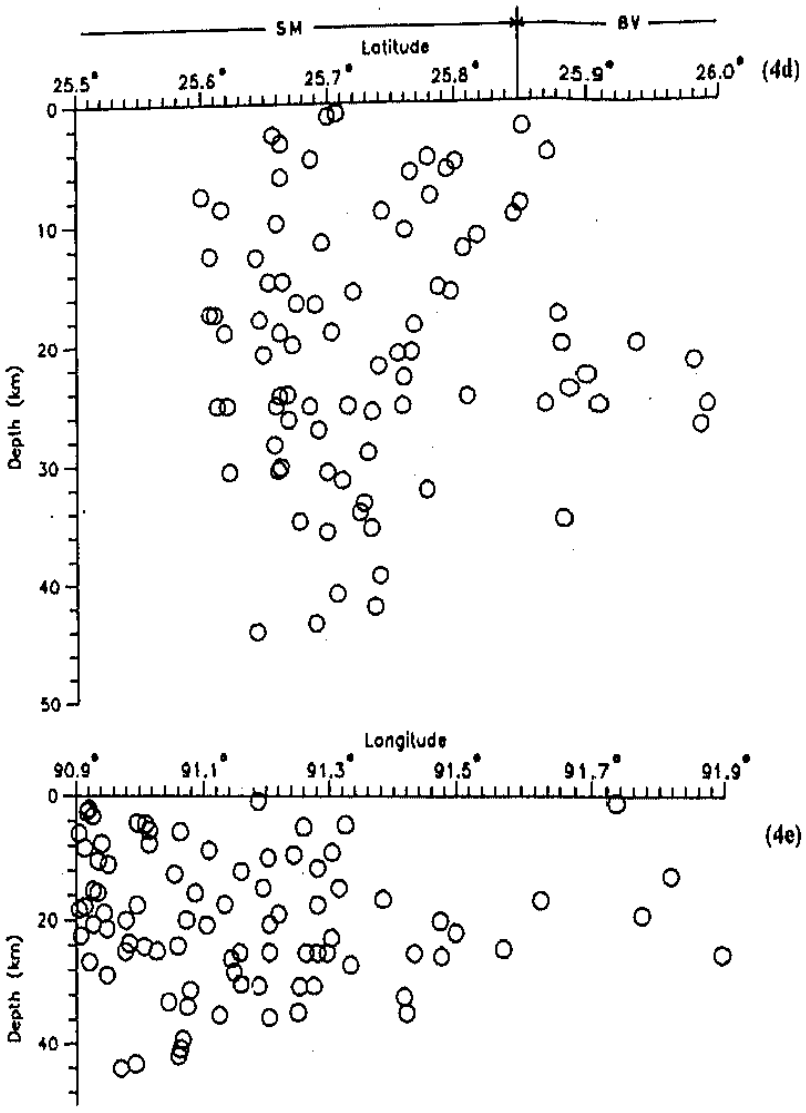

Figure 4. The 1:1 depth sections for earthquakes occurring along different zones in figure 3b. Abbreviations: DDF – Dudhani fault; SM – Shillong massif; BV – Bramhaputra valley. (a) The E-W depth section for zone 1; (b) The N-S depth section for zone 2; (c) The E-W depth section for zone 2; (d) The N-S depth section for zone 3 east of 90·9°E in figure 3; (e) The E-W depth section for zone 3 east of 90·9°E in figure 3.

depth used for locating these earthquakes is 25 km, this clustering is not due to the effect of fixed depth solution. The value of depth for fixed depth solution is 25 km. This clustering occurs right below the boundary between the two seismic velocity layers obtained by us (table 1, Mukhopadhyay 1990). The earthquakes in zone 1 seem to be occurring along a steeply dipping plane as there is hardly any spread of epicenters in N-S direction.

Figures 4b and 4c are the N-S and E-W sections (1:1) of the N-S epicentral trend (zone 2, figure 3b). The cluster observed on the southern portion of zone 2 shows further clustering in 7 to 14 km depth range. Otherwise from these two depth sections it is observed that along zone 2 the earthquakes are fairly diffused in depth as well as in E-W and N-S directions. Most of the earthquakes along zone 2 occur above 30 km depth.

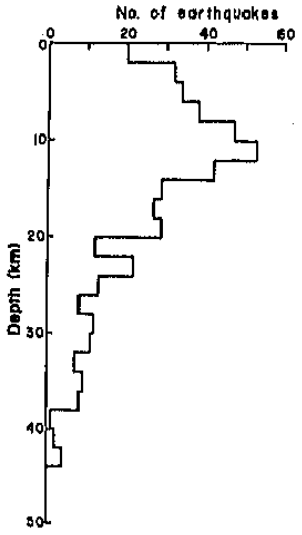

Figure 5. Plot of number of microearthquakes occurring in each 2 km depth interval within the array.

Figures 4d and 4e are the N-S and E-W sections (1:1) of the epicentral trend along zone 3. The earthquakes with deepest focus located by us occur along this trend (depth upto about 45 km). Along this trend the earthquakes show a general tendency of shallowing up towards north (figure 4d) and east (figure 4e).

From the N-S depth section of zone 2 (figure 4b) the inference that can be drawn is that the maximum depth of occurrence of earthquakes in the Shillong massif shows a tendency of increasing towards north. Whereas the depth sections for zone 3 (figures 4d and 4e) show that it decreases towards north and east. The E-W depth sections for zones 2 and 3 (figures 4c and 4e respectively) show that around longitude 90.9°E the earthquakes in zone 3 occur at a deeper level compared to that in zone 2. Thus different seismic zones possess different spatial characteristics.

The plot of a number of earthquakes occurring within the array in each 2 km depth interval and located with rms error less than or equal to 1·0s is shown in figure 5. We see from this figure that the maximum number of earthquakes (90%) occurred in the top 30 km depth. The peak number of earthquakes is confined between the depth of 8 to 14 km depth.

4.4 *Composite fault plane solutions*

A composite fault plane solution should be based on first motion data from carefully selected earthquakes having a good probability of occurring on similar fault planes. Therefore, we have chosen a group of earthquakes lying in a linear zone for drawing a composite fault plane solution. As the Shillong massif is crisscrossed by numerous small faults and fractures these zones should be as narrow and as small as possible. On this basis four groups of earthquakes were considered within an area of 45 km by 70 km (figure 6).

In figure 6 the composite fault plane solutions are represented as beach balls and are superimposed on the seismicity map for better correlation. The solution parameters are given in table 2. A detailed discussion for each solution follows.

The composite fault plane solution (lower hemisphere) for the earthquakes in the E-W linear trend (zone 1, figures 3b and 6) shows thrust faulting (figure 7a, table 2).

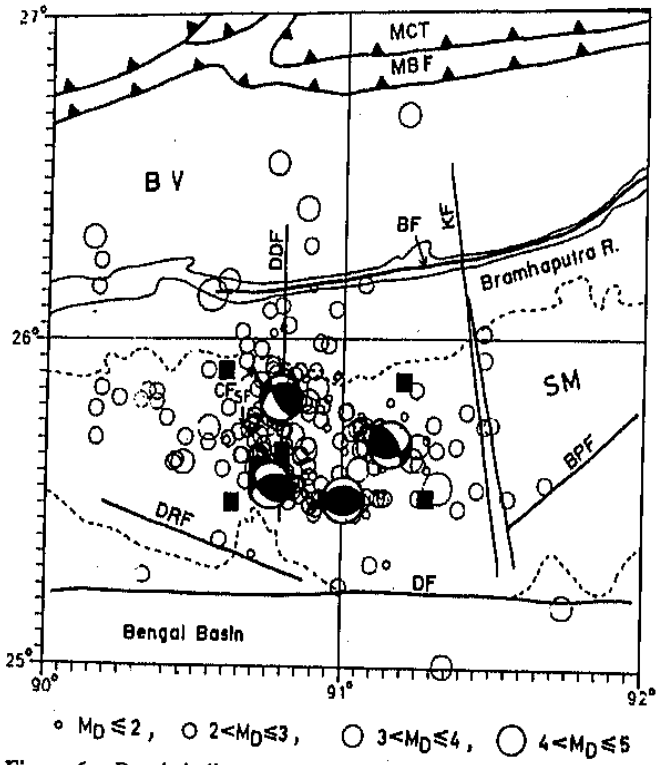

Figure 6. Beach ball representation of the composite fault plane solutions superimposed over the respective clusters of earthquakes for which the solutions are obtained.

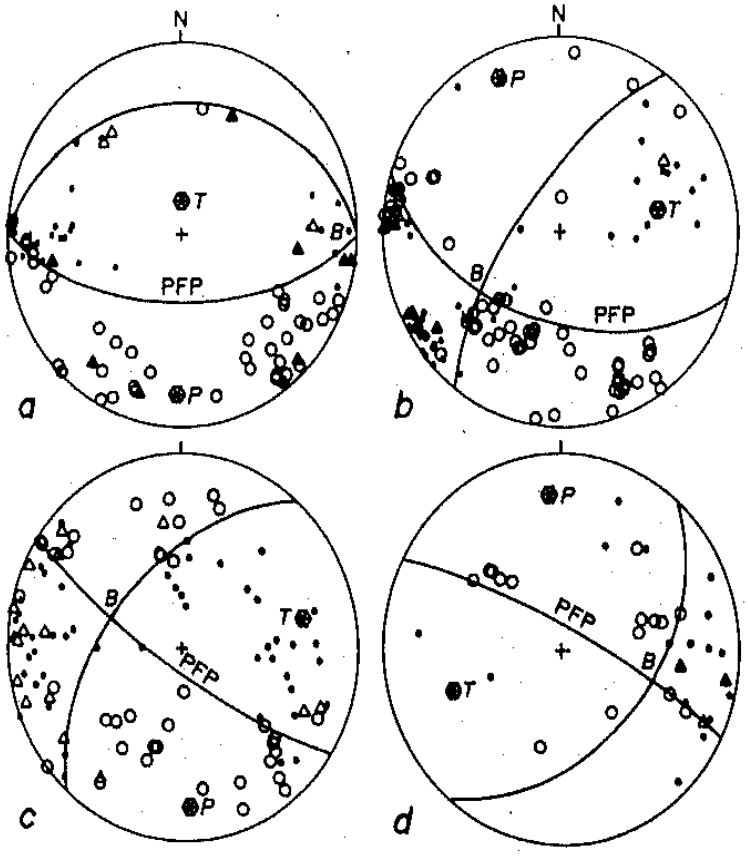

Figure 7. Composite fault plane solutions for earthquakes occurring along different zones shown in figure 3b. (a) For zone 1; (b) For the southern cluster of zone 2; (c) For the northern cluster of zone 2, and (d) For zone 3 in figure 3b.

Table 2. Source parameters obtained by composite fault plane solutions for microearthquakes of Shillong massif. See figures 6 and 7 for comparison. Zone numbers are as given in figure 3b. Zone 2a represents southern cluster of zone 2 and zone 2b represents northern cluster of zone 2.

Zones	Nodal planes						P axis		T axis	
	Plane 1			Plane 2			PA	PD	PA	PD
	S	DA	DD	S	DA	DD				
1	N92°	60°	N182°	N92°	30°	N2°	16°	N182°	74°	N2°
2a	N36°	72°	N306°	N110°	50°	N200°	14°	N338°	44°	N80°
2b	N42°	56°	N312°	N124°	80°	N214°	16°	N177°	31°	N77°
3	N38°	48°	N128°	N119°	80°	N28°	20°	N355°	37°	N250°

Note: S – strike; DA – amount of dip; DD – dip direction; PA – amount of plunge; PD – plunge direction.

The nodal planes trend in almost E-W direction. The strike of the nodal planes is parallel to that of the Dauki fault. The earthquakes occurring along this E-W trending zone show very little spread in N-S direction (figure 3b) indicating the fact that the fault plane on which they occurred was steeply dipping. We, therefore take the first plane (table 2) dipping towards south having a steeper dip to be the fault plane.

The N-S trend (zone 2) in figure 3b shows two clusters in the epicentral plot. The composite fault plane solution of the southern cluster (figure 6) having greater intense activity is shown in figure 7b. It shows strike slip movement with reverse component (table 2). The second nodal plane is subparallel to the NW-SE trending Dapsi reverse fault and shows right lateral movement. We prefer this as the fault plane.

The northern portion of the N-S trend (zone 2) also shows strike slip faulting with reverse component (figure 7c). The second nodal plane is subparallel to the Dapsi reverse fault (figures 3b and 6) and parallel to zone 3 and also shows right lateral movement. Although the above two fault plane solutions are for earthquakes occurring around Dudhani fault, the nodal planes are more parallel to the Dapsi reverse fault present SW of Dudhani fault, which shows a trend parallel to the overall seismicity pattern (figure 3a).

Most of the earthquakes occurring along zone 3 east of 91°E (figures 3 and 6) occur at a deeper level and show up as a thin linear dipping band in the E-W depth section (figure 4e). The composite fault plane solution for this data set is shown in figure 7d (table 2). There are relatively fewer data points in this case. Consequently this solution is not very well constrained. The second nodal plane is parallel to the epicentral trend of these earthquakes and the Dapsi reverse fault (figure 6) and that is why we prefer to call it the fault plane. The sense of motion along this plane is right lateral.

A significant result obtained from all the fault plane solutions considered by us is the remarkable uniformity of orientation of the P axis (figures 7a to 7d, table 2). For all the solutions P axes are oriented almost in N-S direction and have shallow plunge ($< 20°$). The T and B axes, however, change directions. We, therefore, propose that the maximum compressive stress axis (P axis) is oriented in roughly N-S direction in this region.

Kayal (1987) and Kayal and De (1991) have treated this whole area as one group and come up with a dominant thrust fault mechanism with the maximum compressional

stress axis (P axis) in the ENE-WSW direction. This discrepancy in their and our results may be because earthquakes belonging to different fault planes were grouped together in one composite solution by them.

5. Discussion

The seismicity shows WNW-ESE trend (figure 3a). Most of the fault plane solutions also show a similar trend of the inferred fault planes. Similar trend is also observed in the epicentral location given by Gupta *et al* (1986) for earthquakes occurring over the NE corner of the Bengal basin and in the epicentral location and nodal planes of fault plane solutions of some well located earthquakes across this part given by Chen and Molnar (1990).

The microearthquakes show linear patterns in the epicentral plot (figure 3b). They trend in NE, NW, and N-S direction. Similar trends are also seen in the numerous geologically observed faults and fractures occurring within the massif. Among all the existing faults within or near the array the N-S trending Dudhani fault was the most active one during the early part of 1984. Activity was also observed along linear zones parallel to Dauki fault and to Dapsi reverse fault. However, these zones were offset from the fault locations by about 25 km and 50 km respectively.

Earthquakes along different zones occurred upto different depth levels. Along zone 1 they occurred upto 25 km depth, along zone 2 they occurred up to 30 km depth and along zone 3 they occurred up to about 45 km depth (figures 4a to 4e). Kayal (1987) and Kayal and De (1991) show that in this area earthquakes occur upto about 30 km depth. Chen and Molnar (1990) show that some well-located earthquakes in this area have depth of foci of about 50 km.

A plot of variation of frequency of earthquakes with depth is a very good indicator of the depth extent upto which the crust behaves elastically. The elastic part of upper crust is defined as the seismogenic zone by Sibson (1982, 1986), Anderson *et al* (1983), and Chen and Molnar (1983). This is a zone in which 90% of the earthquakes in a region occur (Sibson 1982). According to them due to increase in temperature, rocks undergo quasielastic deformation below a certain depth and cannot store enough elastic strain to have a large number of earthquakes or big earthquakes. The maximum amount of shear strain accumulates at the transition between the more elastic seismogenic zone on top and the quasielastic zone below it where some ductile deformation also takes place. Larger magnitude ($M > 5{\cdot}5$) earthquakes usually nucleate towards the base of the zone of inferred peak shear resistance that lies at the base of the seismogenic zone.

According to this definition the base of the seismogenic zone should lie at 30 km depth in the Shillong massif. However, that seems to be too large a depth for the 1897 great Assam earthquake. This is because the detailed and meticulous field investigation carried out by Oldham (1899) and his deputies in the epicentral tract of this earthquake suggested a much shallower depth of source.

Our data and those by Kayal (1987) and Chen and Molnar (1990) suggest that the crust and the upper mantle in this area behaves elastically and the base of the seismogenic zone should lie at 30 km depth. We observe that the frequency of earthquakes versus depth show a peak within 8-14 km depth range. Bles and Fenga (1986) say, "It is generally observed that small faults and microfaults become more

numerous in the vicinity of large mapped faults" (p. 106). This would mean that more microearthquakes should occur near the vicinity of large faults. From this discussion we suggest that the 1897 great Assam earthquake may have occurred in the 8-14 km depth range

The velocity model of this region obtained by analysis of microearthquake data (Mukhopadhyay 1990; table 1) shows that the top 11·5 $\pm$ 0·5 km consists of a homogeneous layer, whereas the next 14·0 $\pm$ 0·5 km is more heterogeneous. Though data indicate the presence of heterogeneous zone, the nature of heterogeneity is not uniquely determined. On the basis of model analysis Mukhopadhyay (1990) suggested that possibly, this heterogeneous region is made up of thin layers interspersed with slices of low velocity material. We propose that such a structure has developed due to overthrusting of the massif along a fault plane located at the boundary between these two layers and slip may have occurred along that plane during the above mentioned earthquake. From the above discussions the probable depth of this fault plane may be further constrained at around 11 to 12 km.

The large scale damage and deformation over a wide area as well as observation of surface waves due to this earthquake (Oldham 1899) also lead us to suggest that this earthquake had a shallow origin.

We note that a significant number of earthquakes ($\approx$ 10%) occur within 30–45 km depth range in this area. Most of the microearthquakes occurring below 30 km lie along zone 3 (figures 3b, 4d, and 4e). According to Chen and Molnar (1990) there is a paucity of earthquakes in the 30–50 km depth range in north east India. They suggest that this is an aseismic zone sandwiched between the elastic upper crust and a cold upper mantle. From our and Chen and Molnars' data we suggest that there may not be any aseismic zone in this depth range, i.e. even the lower crust is seismically active. We however note that most of the earthquakes analysed by Chen and Molnar occur SE of the Shillong massif, mostly below the Tripura fold belt and the Arakan Yoma ranges.

Chen and Molnar (1990) propose the possibility that lithosphere here is colder than normal because even the upper mantle in this region behaves elastically. Heat flow data for the massif is not available. However, those available for the areas immediately around the massif show a slightly below normal amount of heat flow (Panda 1985; Shanker 1988).

We suggest from this study that in Shillong massif rocks behave elastically up to about 45 km depth. As a consequence a large number of small antithetic faults and fractures have developed both above and below the megathrust on which the 1897 earthquake occurred. They form steeply dipping active zones as observed from depth sections and fault plane solutions presented in this study. According to geological evidences (Bles and Fenga 1986) such a relation between a major fault and associated minor faults is possible.

The composite fault plane solution (figure 7a) for the E-W trending epicentral zone (zone 1, figure 3b) shows pure thrust mechanism. For this case the epicentral trend and the nodal planes are parallel to the Dauki fault. Whereas for a trend that lies at an angle to this trend the solutions (figures 7b to d) show strike slip mechanism with thrust component. The preferred fault planes are all parallel to the Dapsi reverse fault and to the general epicentral trend seen in this region (figure 3a). The variation in fault mechanism may have occurred due to diverse orientation of pre-existing faults with respect to the prevalent tectonic stress in the area.

The most reliable solutions obtained for earthquakes in the eastern Himalaya display northward underthrusting of the Indian plate (Fitch 1972; Chandra 1975, 1978, 1981; Verma *et al* 1976; Le Dain *et al* 1984; Ni and Barazangi 1984; Baranowiski *et al* 1984). The P axes are oriented in N-S direction, i.e. perpendicular to the Himalayan arc. The fault plane solutions in the Arakan Yoma however are dominantly strike slip with P axis oriented in a N-S direction parallel to the N-S folds characterizing E-W crustal shortening. There is an absence of thrust fault earthquakes along these ranges (Chandra 1975; Mukhopadhyay 1984; Le Dain *et al* 1984; Mukhopadhyay and Dasgupta 1988; Chen and Molnar 1990). This evidence has been used by Le Dain *et al* (1984) to propose that eastward subduction is no longer active in the Arakan Yoma ranges and the entire Indian plate now moves northward causing strike slip faulting in this area. The P axis orientation for earthquakes occurring in and around the Shillong massif is roughly N-S (Chen and Molnar 1990; Chandra 1975; Mukhopadhyay 1990) indicating that this region too experiences the effect of predominantly northward movement of the Indian plate.

6. Conclusions

To propose an active tectonic model of this area based on seismic data, one has to explain the process causing the present-day seismicity as well as the genesis of the 1897 great Assam earthquake that occurred here. This has been done in the previous section and on the basis of it we propose that:

- The thrust plane on which the 1897 great Assam earthquake of magnitude 8·7 occurred lies within the depth range 11–12 km. In this work for the first time the depth of this earthquake has been estimated on the basis of independent data other than Oldham's report (1899).
- The steeply dipping faults and fractures within the massif and the Dauki fault are antithetic faults present around the thrust plane. Minor movements along these faults cause microearthquakes. That is why the seismicity shows a widespread distribution in depth rather than showing a clustering around the thrust plane. The antithetic faults have steep dip. That is why the microearthquakes are seen to be occurring along steeply dipping linear zones and the fault plane solutions show steep nodal planes. Some of these faults above and below the megathrust may have very little or no lateral separation making them look like steeply dipping zones cutting across the megathrust.
- The antithetic faults could develop below the thrust plane along which movement occurred during the 1897 great Assam earthquake because this region also behaves elastically. Chen and Molnar (1990) opined that the lithosphere here is colder than normal and even the upper mantle behaves elastically. From heat flow data Panda (1985) and Shanker (1988) found that the crust in this area is colder than average crust. Our findings give further support to this view.
- At present the massif is experiencing N-S directed compression.

Acknowledgement

This work was sponsored by the Department of Science and Technology under the project 'All India Coordinated Project in Himalayan Seismicity', and the University

Grants Commission under the project 'Special Assistance Program in Engineering Geosciences'.

References

Anderson J L, Osborne R H and Palmer D F 1983 Cataclastic rocks of the San Gabriel fault – an expression of deformation at deeper crustal levels in the San Andreas fault zone; *Tectonophysics* **98** 209–251

Auden J B 1972 Review of the tectonic map of India published by O.N.G.C.; *J. Geol. Soc. India* **13** 101–107

Bles J L and Fenga B 1986 Relationships between large and small fractures; In: *The fracture of rocks* (translated by) Wanklyn J (France: North Oxford Academic) pp. 105–112

Chandra U 1975 Seismicity, earthquake mechanisms and tectonics of Burma, 20°N–28°N; *Geophys. J. R. Astron. Soc.* **40** 367–381

Chandra U 1978 Seismicity, earthquake mechanisms and tectonics along the Himalayan mountain range and vicinity; *Phys. Earth Planet. Inter.* **16** 109–131

Chandra U 1981 Focal mechanism solutions and their tectonic implications for the eastern Alpine-Himalayan region; In: Zagros, Hindukush, Himalaya, Geodynamic Evolution (eds) H K Gupta and F M Delany, *Geodynamic Series v.* 3 pp. 243–271

Chen W P and Molnar P 1983 Focal depths of intracontinental and intraplate earthquakes and their implications for the thermal and mechanical properties of the lithosphere; *J. Geophys. Res.* **88** 4183–4214

Chen W P and Molnar P 1990 Source parameter of earthquakes and intraplate deformation beneath the Shillong plateau and the northern Indoburman ranges; *J. Geophys. Res.* **95** 12527–12552

Evans P 1964 The tectonic framework of Assam; *J. Geol. Soc. India* **5** 80–96

Fitch T J 1972 Plate convergence, transcurrent faults, and internal deformation adjacent to southeast Asia and the western Pacific; *J. Geophys. Res.* **77** 4432–4460

Gehalaut V K and Chander R 1992 A rupture model for the great earthquake of 1897, NE India, and its geodynamic and seismic hazard implication; *Tectonophysics* (accepted)

GSI 1974 Geology and mineral resources of the states of India; *Geol. Surv. India, Misc. Publ.* **30** 1–124

Gupta H K, Rajendran K and Singh H N 1986 Seismicity of the north-east India region. Part I: The data base; *J. Geol. Soc. India* **28** 345–365

Gupta R P and Sen A K 1988 Imprints of the ninety-east ridge in the Shillong plateau, Indian shield; *Tectonophysics* **154** 335–341

Kayal J R 1987 Microseismicity and source mechanism study: Shillong plateau, northeast India; *Bull. Seismol. Soc. Am.* **77** 184–194

Kayal J R and De R 1991 Microseismicity and tectonics in northeast India; *Bull. Seismol. Soc. Am.* **81** 131–138

Kharshiing A D 1985 *Neotectonics and crustal structure in Shillong massif and neighbouring regions*; Unpublished M. Tech. thesis, Univ. of Roorkee pp. 58

Khattri K N, Chander R, Mukhopadhyay S, Sriram V and Khanal K N 1992 A model of active tectonics in the Shillong massif region; In: *The Himalayan Orogen and Global Tectonics* (ed) A K Sinha, (Delhi: Oxford & IBH) pp. 205–222

Khattri K N 1987 Great earthquakes, seismicity gaps and potential for earthquake disaster along the Himalaya plate boundary; *Tectonophysics* **138** 79–92

Le Dain A Y, Tapponier P and Molnar P 1984 Active faulting and tectonics of Burma and surrounding regions; *J. Geophys. Res.* **89** 453–472

Lee W H K and Lahr J C 1975 HYPO71 (revised): a computer program for determining hypocenter, magnitude and first motion pattern of local earthquakes; *Geol. Surv. Open-File Rep. (U. S.)* **75–311** 1–116

Molnar P 1987 The distribution of intensity associated with the great 1897 Assam earthquake and bounds on the extent of the rupture zone; *J. Geol. Soc. India* **30** 13–27

Mukhopadhyay M 1984 Seismotectonics of transverse lineaments in the eastern Himalaya and its foredeep; *Tectonophysics* **109** 227–240

Mukhopadhyay M and Das Gupta S 1988 Deep structure and tectonics of the Burmese arc: constraints from earthquake and gravity; *Tectonophysics* **149** 299–322

Mukhopadhyay S 1990 *Seismic velocity structure and seismotectonics of the Shillong massif, north eastern India*; Unpublished Ph. D. thesis, Univ. of Roorkee, pp. 247

Murthy M V N 1970 Tectonic and mafic igneous activity in north-east India in relation to Upper Mantle; *Proc. 2nd Symp. Upper Mantle Projects.* Dec. 1970 Hyderabad, pp. 287–304

Murthy M V N, Talukdar S C, Bhattacharya and Chakraborty 1971 The Dauki fault of Assam; *Bull. O.N.G.C.* 6 57–64

Nandy D R and Dasgupta S 1986 Application of remote sensing in regional geological studies – a case study in the northeastern part of India; *Proc. Int. seminar on photogrammetry and remote sensing for developing countries*, New Delhi, March 1986 1(T.4) pp. 6·1–6·9

Ni J and Barazangi M 1984 Seismotectonics of the Himalayan collision zone: Geometry of the under-thrusting India plate beneath the Himalaya; *J. Geophys. Res.* 89 1147–1163

Nicholson C and Simpson D W 1985 Changes in V_P/V_S with depth: Implications for appropriate velocity models, improved earthquake locations, and material properties of the upper crust; *Bull. Seismol. Soc. Am.* 75 1105–1123

Oldham R D 1899 Report on the great earthquake of 12th June 1897; *Mem. Geol. Surv. India* 29 379

Panda P K 1985 Geothermal maps of India and their significance in resources assessments. In: *Petroleferous Basins of India III* Special vol. of *Petro. Asia J.* 3 202–210

Pascoe E H 1950 A manual of the Geology of India and Burma; *Geol. Surv. India Publ.* 1 483

Riznichenko Y V 1958 Methods for large-scale determination of focus coordinates of nearby earthquakes and velocities of seismic waves in the focal region; *Tr. Inst. Fiz. Zemli. Akad. Nauk. SSSR* 4 321

Seeber L, Armbruster J G and Quittmeyer R C 1981 Seismicity and continental subduction in the Himalayan arc; In: Zagros, Hindukush, Himalaya, Geodynamic evolution (eds) H K Gupta and F M Delany Geodynamic Series 3, pp. 215–242

Shanker R 1988 Heat-flow map of India and discussions on its geological and economic significance; *Indian Minerals* 42 89–110

Sibson R H 1982 Fault zone models, heat flow, and the depth distribution of earthquakes in the continental crust of the United States; *Bull. Seismol. Soc. Am.* 72 151–163

Sibson R H 1986 Earthquakes and rock deformation in crustal fault zones; *Annu. Rev. Earth Planet. Sci.* 14 149–175

Verma R K and Mukhopadhyay M 1977 An analysis of the gravity field in northeastern India; *Tectonophysics* 42 283–317

Verma R K, Mukhopadhyay M and Ahluwalia M S 1976 Seismicity, gravity, and tectonics of northeast India and northern Burma; *Bull. Seismol. Soc. Am.* 66 1683–1694

Wadati K 1933 On the travel time of earthquake waves. Part II; *Geophys. Mag.* 7 101–111